Biochemistry
Article
Cite This: Biochemistry XXXX, XXX, XXX−XXX
pubs.acs.org/biochemistry

Selectivity within a Family of Bacterial Phosphothreonine Lyases

Kaitlin A. Chambers, Nile S. Abularrage, and Rebecca A. Scheck*

Department of Chemistry, Tufts University, 62 Talbot Avenue, Medford, Massachusetts 02155, United States

Supporting Information

ABSTRACT: Phosphothreonine lyases are bacterial effector proteins secreted into host cells to facilitate the infection process. This enzyme family catalyzes an irreversible elimination reaction that converts phosphothreonine or phosphoserine to dehydrobutyrine or dehydroalanine, respectively. Herein, we report a study of substrate selectivity for each of the four known phosphothreonine lyases. This was accomplished using a combination of mass spectrometry and enzyme kinetics assays for a series of phosphorylated peptides derived from the mitogen-activated protein kinase (MAPK) activation loop. These studies provide the first experimental evidence that VirA, a putative phosphothreonine lyase identified through homology, is indeed capable of catalyzing phosphate elimination. These studies further demonstrate that OspF is the most promiscuous phosphothreonine lyase, whereas SpvC is the most specific for the MAPK activation loop. Our studies reveal that phospholyases are dramatically more efficient at catalyzing elimination from phosphothreonine than from phosphoserine. Together, our data suggest that each enzyme likely has preferred substrates, either within the MAPK family or beyond. Fully understanding the extent of selectivity is key to understanding the impact of phosphothreonine lyases during bacterial infection and to exploiting their unique chemistry for a range of applications.

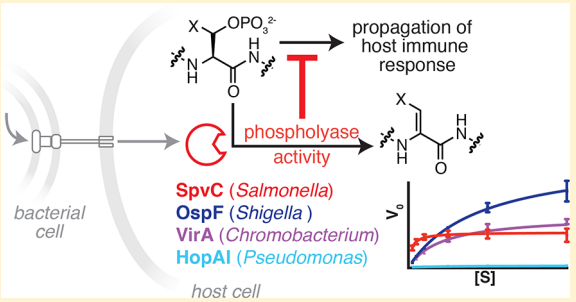

Bacterial effector proteins are key enablers of infection and act through diverse chemical interactions outside and within a host cell.[1−8] Many effector proteins can chemically modify host proteins to interrupt or rewire host signaling pathways, thereby promoting bacterial survival and replication.[1−5,8] Among these, a subset of effector proteins has been shown to promote transformations that are not found naturally within the mammalian proteome.[9−12] One such example is the elimination of phosphate from phosphorylated serine and threonine residues catalyzed by a family of bacterial phosphothreonine lyases (also termed phospholyases). This modification generates the electrophilic Michael-like acceptors, dehydroalanine (Dha) and dehydrobutyrine (Dhb), in place of phosphoserine and phosphothreonine, respectively (Figure 1A,B).[9,10,13−15] Unlike phosphatases, which catalyze the reversible removal of phosphate through hydrolysis, phosphothreonine lyases promote an irreversible elimination of phosphate that drastically disrupts endogenous signaling pathways, leaving host cells vulnerable to bacterial infection.[10,12,16] It has been previously established that phosphothreonine lyases target activated, phosphorylated kinases within the mitogen-activated protein kinase (MAPK) pathway, which is a central hub in innate immune signaling.[10,12] Disruption of MAPK signaling through the irreversible removal of phosphate ultimately enables bacteria that secrete phosphothreonine lyases to subvert the host's innate immune response.[17]

Phosphothreonine lyases have been identified in a small number of pathogenic Gram-negative bacteria. These include SpvC from *Salmonella enterica* Typhimurium, OspF from *Shigella flexneri*, VirA from *Chromobacterium violaceum*, and HopAI from *Pseudomonas syringae*.[9,10,12,13] These four phospholyases and their isoforms, which are the only ones to be recognized to date, share high levels of homology. Multiple-sequence alignment illustrates that all of the residues thought to play a role in substrate docking and catalysis are fully conserved within this enzyme family (Figure 1C and Figure S1).[13−15]

Past proteomics studies have found that exposure to *S. flexneri* leads to dramatic, widespread changes in host phosphorylation, affecting hundreds of proteins.[18,19] Additional work has suggested that many of these changes in phosphorylation are mediated by the OspF-dependent silencing of the central MAPK signaling hub.[18] However, these studies evaluated only changes in phosphorylation and did not explicitly monitor the formation of Dhb or Dha. As a result, they do not rule out the possibility that OspF, and other phospholyase family members, act on a broad range of targets to eliminate phosphate from many phosphorylated host proteins. As phosphoserine and phosphothreonine comprise roughly 99% of the native phosphoproteome,[20] understanding the extent of selectivity or promiscuity within the phosphothreonine lyase family is a crucial step toward identifying their complete repertoire of substrates and subsequent effects on host biochemical processes during bacterial infection. A complete understanding of such differences in selectivity could be useful for the identification of unique biomarkers for bacterial infection and has the potential to lead to the development of new antibiotic interventions.

Herein, we report on the substrate selectivity for each member of the phosphothreonine lyase family. To do so, we prepared

Received: May 9, 2018
Published: May 24, 2018

DOI: 10.1021/acs.biochem.8b00534
Biochemistry XXXX, XXX, XXX−XXX

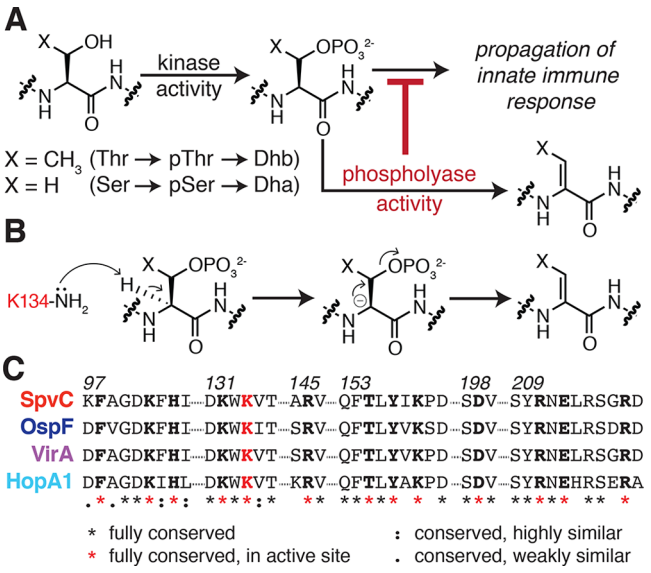

Figure 1. (A) Bacterial phosphothreonine lyases catalyze the irreversible elimination of phosphate from phosphothreonine (pThr) or phosphoserine (pSer) to generate dehydrobutyrine (Dhb) or dehydroalanine (Dha), respectively. This enables bacteria to silence host phosphorylation cascades and to subvert the host immune response. (B) Proposed catalytic mechanism for phospholyase-catalyzed phosphate elimination through an $E1_{CB}$ mechanism. (C) Multiple-sequence alignment illustrates the high level of homology shared by all four members of the phosphothreonine lyase family, particularly within and surrounding the active site (shown).

point mutations to a phosphothreonine-containing peptide derived from the MAPK activation loop. Using a combination of mass spectrometry and enzyme kinetics assays, we demonstrate that OspF is the most promiscuous member of the phosphothreonine family, whereas SpvC is the most specific for the MAPK activation loop. We also confirm experimentally that VirA is a phosphothreonine lyase, capable of catalyzing phosphate elimination. These data suggest that phosphothreonine lyases, especially OspF, act on additional substrates in host cells, both within and outside the MAPK family.

METHODS

General. All chemical reagents were of analytical grade, obtained from commercial suppliers, and used without further purification unless otherwise noted. Water used in biological procedures was distilled and deionized using an Arium pro purification system (Sartorius).

Enzyme Expression and Purification. An *Escherichia coli* optimized copy of each phospholyase gene was cloned into the pRSET A vector, which fuses target proteins with an N-terminal His-tag to be used for purification. Expression vectors encoding OspF, SpvC, and VirA were transformed into BL21-CodonPlus-RIL (Agilent) *E. coli*. Cultures were grown to an OD_{600} of 0.6 at 37 °C, and expression was induced with 0.1 mM isopropyl β-D-1-thiogalactopyranoside (IPTG) at 20 °C for 3 h. Because of solubility issues, the expression vector encoding HopAI was transformed into OverExpress C41(DE3) (Lucigen) *E. coli* and grown to an OD_{600} of 0.6 at 37 °C, and expression was induced with 0.3 mM IPTG at 20 °C for 18 h. After expression, cells were pelleted and frozen. BugBuster protein extraction reagent was used along with 0.5 mM phenylmethanesulfonyl fluoride and Benzonase nuclease to lyse bacterial cells. Proteins were purified using the His-GraviTrap protein purification column eluting with imidazole-Tris-buffered saline [500 mM imidazole, 100 mM Tris, and 50 mM NaCl (pH 7)]. A buffer exchange was performed using Tris-buffered saline [100 mM Tris and 50 mM NaCl (pH 7)] to remove imidazole. The resulting pure protein samples were stored at −20 °C. Concentrations were determined using a Bio-Rad Bradford Protein Assay and a Tecan Spark 10M microplate reader.

Peptide Synthesis. Amidated peptides were synthesized using Rink Amide MBHA resin (100−200 mesh, Novabiochem) on a 0.05 mmol scale following standard FMOC synthesis. Coupling steps were accomplished using 5 equiv of amino acid in dimethylformamide (DMF) with *O*-(benzotriazol-1-yl)-*N*,*N*,*N*′,*N*′-tetramethyluronium hexafluorophosphate (HBTU, 5 equiv) and *N*,*N*-diisopropylethylamine (DIPEA, 10 equiv) for 1 h. Phospho-amino acid coupling was extended to 3 h. Synthesis was completed in iterative cycles of FMOC deprotection (20% piperidine in DMF, 2 × 20 min) and coupling, with washes between the steps (4 × 1 min, DMF). Cleavage for phosphothreonine-containing peptides was performed for 3 h with no unexpected side products. Partial cleavage for phosphoserine-containing peptides was performed for 1 h, with unexpected side products forming at longer time points. The resulting solution was then concentrated under an air flow and redissolved in a water/acetonitrile mixture. A list of all peptides synthesized along with their expected and observed masses can be found in Table S1.

Peptide Purification. Peptides were purified on an Agilent 1260 Infinity LC system using a water/acetonitrile mobile phase containing 0.1% TFA and an Agilent ZORBAX SB-C18 column. Peptides were characterized using a Bruker Microflex matrix-assisted laser desorption ionization time-of-flight (MALDI-TOF) mass spectrometer and an Agilent 6530 quadrupole time-of-flight (Q-TOF) mass spectrometer coupled to an Agilent 1260 high-performance liquid chromatography (HPLC) system. Pure fractions were combined and lyophilized, and then each was prepared as a stock peptide solution (10 mM) in water.

Mass Spectrometry. Reversed-phase chromatography and mass spectrometry were performed on an Agilent 1260 Infinity LC system in line with an Agilent 6530 Accurate Mass Q-TOF instrument. Reversed-phase chromatography was performed using a ZORBAX 30SB-C8 column (2.1 mm × 100 mm, Agilent) with a water/acetonitrile gradient mobile phase containing 0.1% formic acid (0.4 mL/min; 2% ACN, isocratic from 0 to 1.75 min, 2 to 48% from 1.76 to 16 min). Data analysis was performed using Agilent MassHunter Qualitative Analysis software. Conversion from the phosphorylated parent peak to the eliminated product peak was calculated based on the detected liquid chromatography−mass spectrometry (LCMS) peak volumes, using equations provided in the Supporting Information. Peak volumes are determined using the Molecular Feature Extractor within the Agilent Qualitative Analysis software.

General Protocol for Phosphate Elimination Catalyzed by Phospholyases. Phosphate elimination experiments were conducted using 10 μM enzyme and 1 mM peptide in Tris-buffered saline (100 mM Tris and 50 mM NaCl). All reactions were performed at pH 8 and 26 °C unless otherwise noted. Reactions were initiated upon addition of peptide to the reaction mixture. Reactions were quenched by diluting 5 μL of the sample in 200 μL of 100 mM HCl.

Steady State Kinetics Studies. Steady state kinetic analysis was performed using the commercially available EnzChek Phosphate Assay Kit (ThermoFisher Scientific). All assays were conducted according to the manufacturer's standard

DOI: 10.1021/acs.biochem.8b00534
Biochemistry XXXX, XXX, XXX−XXX

protocol, monitoring absorbance with a Tecan Spark 10M microplate reader. Briefly, increasing concentrations of phosphopeptide were added to a buffered reaction mixture containing 2-amino-6-mercapto-7-methylpurine riboside (MESG) and purine nucleoside phosphorylase (PNP). Reactions were initiated by adding phospholyase (500 nM) to the solution of assay components and substrate peptides in 96-well Costar assay plates (Corning). The rates of reaction were determined at various peptide substrate concentrations based on the absorbance at a λ_{max} of 360 nm. Data were fit to the Michaelis−Menten nonlinear regression in GraphPad Prism.

RESULTS AND DISCUSSION

Evaluating Phosphate Elimination Catalyzed by Bacterial Phosphothreonine Lyases. Previous work has established that the MAPK activation loop is a substrate for OspF, SpvC, and HopAI.[10] Although this activity has been hypothesized for VirA based on sequence homology, to date this has not been demonstrated experimentally.[9] As a result, the activity of each enzyme was assessed using a short peptide containing the MAPK ERK1/2 activation loop sequence, GFLpTEpYV-NH_2 [peptide **1** (Figure 2A)]. Although this peptide does not completely mimic the natural protein substrate, prior work has suggested that phospholyases can modify peptide substrates in addition to proteins.[10] Moreover, the relative ease of peptide synthesis facilitates the evaluation of many different possible substrates *in vitro*. Following expression and purification of each phospholyase, we designed an LCMS-based assay to monitor the conversion of this phosphothreonine (pThr) substrate (peptide **1**) to its eliminated dehydrobutyrine (Dhb) counterpart [peptide $\mathbf{1}^{Dhb}$ (Figure 2B−D)]. Using this approach, both the disappearance of peptide **1** and the emergence of peptide $\mathbf{1}^{Dhb}$ peaks were observed, thus validating that all phospholyases can accept unstructured peptides as substrates. Because phosphopeptides and their nonphosphorylated counterparts are known to have different ionization efficiencies,[21] we report "apparent conversions" that are based on integrated LCMS peaks. However, HPLC was also used to confirm that our apparent conversion calculation matched closely with conversions calculated using integrated HPLC peak areas (Figure S2).

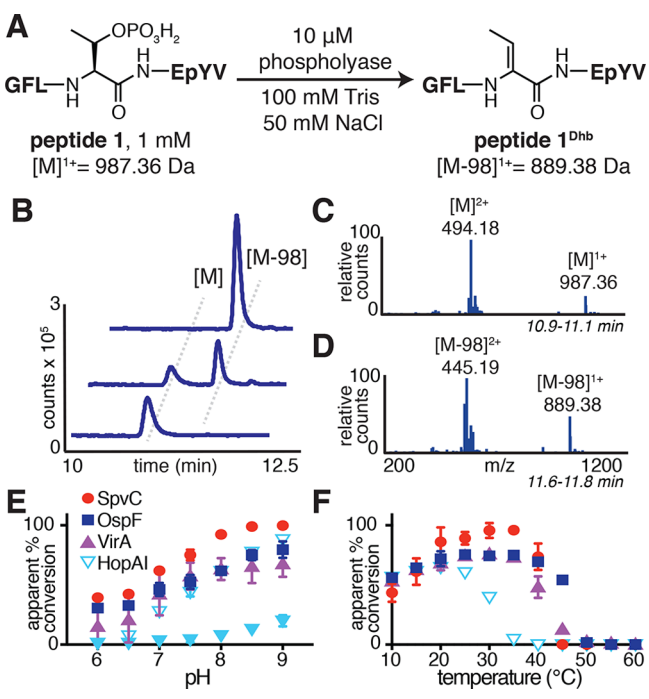

Figure 2. (A) The phospholyase enzyme family catalyzes the elimination of phosphate from phosphothreonine-containing peptides derived from the MAPK activation loop. Phosphate elimination results in a 98 Da mass decrease. (B) Representative chromatogram demonstrating the loss of peptide **1** and the emergence of the product, peptide $\mathbf{1}^{Dhb}$, following phospholyase exposure. MS spectra of (C) peptide **1** and (D) peptide $\mathbf{1}^{Dhb}$. Apparent conversion to peptide $\mathbf{1}^{Dhb}$ determined after incubation for 1 min (filled symbols) with each phospholyase at (E) variable pH at 26 °C and (F) variable temperature at pH 8: SpvC (red), OspF (blue), VirA (purple), or HopAI [cyan; empty cyan triangles represent a longer incubation time (5 min) for HopAI].

Next, this assay was used to evaluate the optimal reaction conditions for each enzyme. As no cofactors are required in this transformation, we simply treated 1 mM peptide **1** with 10 μM enzyme for 1 min. These conditions yielded substantial product formation when peptide **1** was treated with SpvC, OspF, or VirA (Figure 2E). However, low levels of conversion were observed when peptide **1** was incubated with HopAI for 1 min, so longer reaction times (5 min) were used to assess its reactivity (Figure 2E). Reactions were performed across a pH range from 6 to 9 at 26 °C, which is the recommended temperature for culturing *C. violaceum* and *P. syringae*. The results suggest that all four enzymes are most active at pH ≥8 (Figure 2E). This finding is supported by previous literature and is consistent with the elimination mechanism proposed by Ke et al. in which deprotonation of the catalytic lysine residue (Figure 1B) is promoted under basic conditions, thereby enhancing catalysis.[13,15,22] To rule out non-enzymatic elimination, we monitored the extent of reaction in the absence of enzyme and did not observe any elimination even at pH 9 (Figure S3).

Following these experiments, we sought to explore the effect of temperature on phospholyase-catalyzed elimination. It was anticipated that the enzymes from mammalian pathogens (SpvC, OspF, and VirA) would be optimally active at or near the temperature of mammalian host cells. In contrast, HopAI, originating from a plant pathogen, would be expected to have optimal activity at lower temperatures, as plant pathogens typically suppress virulence factors at temperatures above 28 °C.[23] Notably, *Salmonella* spp. can infect both mammalian and plant hosts.[16] At pH 8, it was observed that SpvC, OspF, and VirA tolerate temperatures between 20 and 40 °C, with optimal activity between 25 and 35 °C. In contrast, HopAI has a profile better suited to lower temperatures, 15−30 °C (Figure 2F). We chose to proceed using conditions (26 °C and pH 8) that were both biologically reasonable and within the optimal activity range for each enzyme. This enabled us to compare the performance of all four enzymes directly.

Kinetics Assays for Comparing Phosphothreonine Lyase Activities. The next goal was to determine the kinetic parameters for each of these four phospholyases. To do so, we turned to the commercially available EnzChek assay that couples the release of phosphate, which occurs as peptide **1** is converted to peptide $\mathbf{1}^{Dhb}$ (Figure 3A), to an enzymatic reaction that converts 2-amino-6-mercapto-7-methylpurine riboside (MESG) to 2-amino-6-mercapto-7-methylpurine and ribose 1-phosphate (Figure 3B). This transformation can be monitored by an increase in absorbance at 360 nm as the purine base is liberated (Figure 3C,D). We determined that OspF had the largest k_{cat} value, nearly triple the value obtained for SpvC, and close to

DOI: 10.1021/acs.biochem.8b00534
Biochemistry XXXX, XXX, XXX−XXX

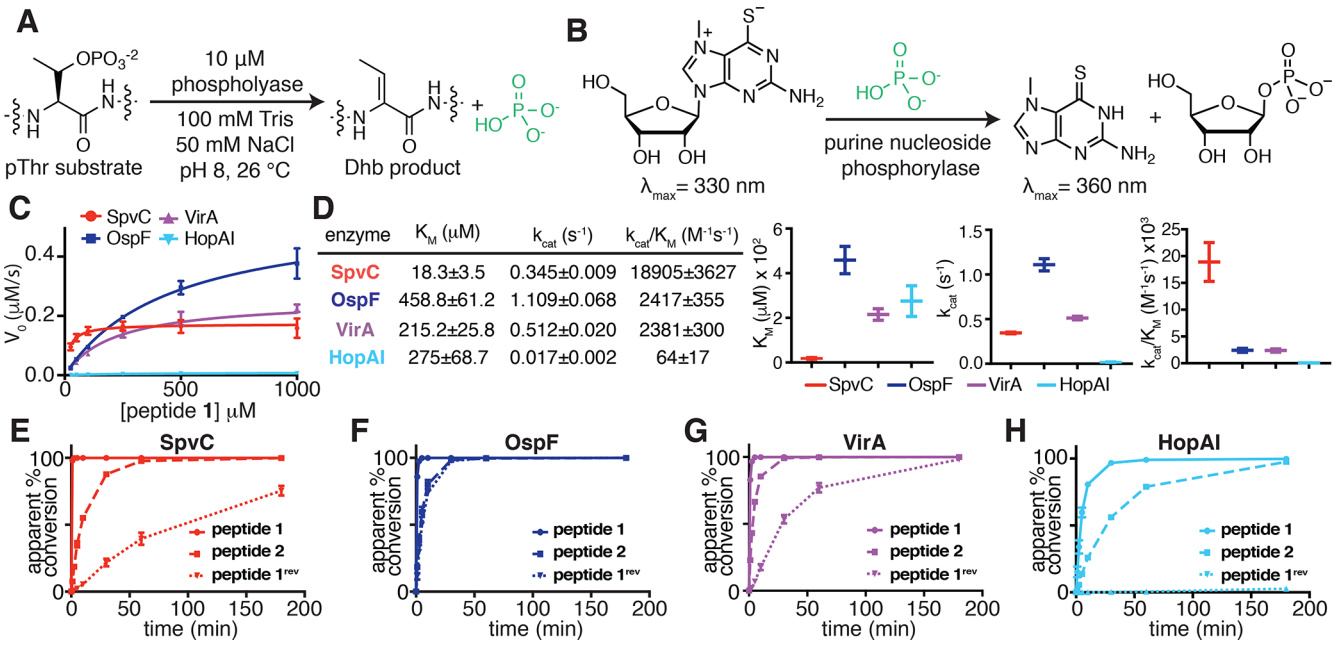

Figure 3. (A) Phosphate is released as phospholyases catalyze the formation of Dhb. (B) Phosphate release can be coupled to the EnzChek assay, which converts MESG to a methyl purine causing a shift in absorbance that is used to quantify the amount of phosphate released. (C) Initial rates of elimination for peptide **1** treated with SpvC (red), OspF (blue), VirA (purple), or HopAI (cyan). (D) Kinetic parameters determined for the elimination of peptide **1** upon treatment with each phospholyase. (E) Time course depicting the conversion of peptide **1** (solid line), peptide **2** (dashed line), and peptide $\mathbf{1}^{rev}$ (dotted line) to their corresponding Dhb products after incubation with SpvC, (F) OspF, (G) VirA, and (H) HopAI.

double that for VirA. HopAI was once again the most sluggish enzyme of the group with the lowest k_{cat} value. In contrast, SpvC was found to have the lowest K_M, followed by VirA, HopAI, and OspF.

The catalytic efficiencies (k_{cat}/K_M) for each enzyme were also examined. SpvC has by far the highest catalytic efficiency, with OspF and VirA having roughly similar, lower efficiencies and HopAI performing the worst of all (Figure 3C,D). These results emphasize that SpvC is the best enzyme for the dually phosphorylated ERK1/2 activation loop (peptide **1**). This further suggests that OspF, despite its weak affinity for MAPK substrates relative to the affinities of the other phospholyases, may have the potential to effectively perform elimination on other substrates because of its high k_{cat}. Furthermore, these data suggest that HopAI could be better suited for a target endogenous to the plant proteome because of its poor performance relative to other family members.

Exploration of Substrate Requirements within the MAPK Activation Loop. Building on these observations, we sought to understand the enzymes' substrate selectivity. Classical MAPK activation loops have a consensus sequence of ~pT-X-pY~,[17,24] and our initial studies utilized the dually phosphorylated ERK1/2 peptide substrate (peptide **1**, pT-E-pY). A variant of this substrate that presented the sequence of the dually phosphorylated ERK1/2 activation loop in reverse (peptide $\mathbf{1}^{rev}$, pY-E-pT) was also prepared, as well as a version that lacks phosphorylation at Tyr (peptide **2**, pT-E-Y). A complete list of peptides used throughout this work can be found in Table S1. We used our LCMS-based assay to determine how these changes to the substrates would be tolerated by each enzyme. First, a time course experiment was performed, which highlights the roughly comparable activities of SpvC, OspF, and VirA while distinguishing HopAI as the most inert of these enzymes toward peptide **1** (solid line, Figure 3E−H). This result is in agreement with those of our kinetics studies. Next, reversing the order of the dually phosphorylated sequence led to a dramatic reduction in the extent of elimination catalyzed by SpvC, VirA, and HopAI [peptide $\mathbf{1}^{rev}$ (Figure 3E−H, dotted line)]. However, in the case of OspF, the decrease in activity was far less pronounced (Figure 3F). It was possible to obtain kinetic parameters for the elimination of peptide $\mathbf{1}^{rev}$ catalyzed by OspF and VirA. Intriguingly, OspF had a lower K_M for peptide $\mathbf{1}^{rev}$ (311 ± 51 μM) than for peptide **1**, though the overall catalytic efficiency was reduced ~5-fold (489 ± 86 M^{-1} s^{-1}). VirA exhibited an increase in K_M along with a decrease in k_{cat}, resulting in a nearly 10-fold decrease in the overall catalytic efficiency (31 ± 31 M^{-1} s^{-1}) (Figure S4A−D and Table S2). Data collected for SpvC and HopAI could not be fit to a Michaelis−Menten curve, as the amount of phosphate released was at or below the lower limit of detection for the assay. Together, these data demonstrate that OspF and VirA are the most tolerant to large changes in the substrate, in this case the reversal of its sequence.

Next, by simply mutating pTyr to Tyr, we observed a significant decrease in the extent of phosphate elimination for all phospholyases [peptide **2** (Figure 3E−H, dashed line, and Figure S4E,F)]. This suggests that the dually phosphorylated activation loop (peptide **1**) is a much better substrate than the monophosphorylated version (peptide **2**). Notably, the activity of SpvC was most sensitive to the change from pTyr to Tyr, as evidenced by the observation that peptide **2** reached 98.1 ± 0.7% conversion only after incubation with SpvC for 1 h. In contrast, 98.0 ± 1.6% conversion was reached after treatment for just 1 min for peptide **1**. Accordingly, SpvC suffered a 15-fold increase in K_M and a 10-fold decrease in k_{cat}. This resulted in a dramatic decrease in catalytic efficiency, equal to 2 orders of magnitude, when catalyzing elimination from peptide **2**, dropping to 113 ± 32 M^{-1} s^{-1} (Figure S4E,F and Table S2). Of the four phospholyases tested, VirA and HopAI were most tolerant to the substitution of the monophosphorylated peptide **2**, as each catalyzed levels of elimination within 10 min that were similar to

DOI: 10.1021/acs.biochem.8b00534
Biochemistry XXXX, XXX, XXX−XXX

those obtained for peptide **1** at 1 min. OspF took just >10 min to catalyze the same levels of elimination for peptide **2** that were attained for peptide **1** at 1 min. Both OspF and VirA suffered a decrease in catalytic efficiency when catalyzing elimination from peptide **2**, falling roughly an order of magnitude from the efficiencies obtained for peptide **1** (250 ± 36 and 278 ± 51 M^{-1} s^{-1}, respectively). These changes in catalytic efficiency were primarily due to increases in K_M; k_{cat} values were also decreased but to a far lesser extent (Figure S4E,F and Table S2). Kinetic parameters for HopAI could not be determined because of the small amounts of phosphate released. Interestingly, OspF catalyzed virtually the same extent of elimination for both peptide **2** and peptide $\mathbf{1}^{rev}$ (Table S2). Together, these results suggest that OspF is far more promiscuous than the other enzymes, perhaps modifying a wider range of substrates.

Investigation of Sequence Requirements at the +2 Position within Phospholyase Substrates. On the basis of MAPK family homology, tyrosine is highly conserved in the +2 position relative to the central threonine (Figure S5);[17,24] both of these residues are phosphorylated when MAPK is activated in response to a stimulus such as bacterial infection. A crystal structure of SpvC bound to a suboptimal MAPK substrate, the doubly phosphorylated ERK5 activation loop (QYFMpTEpY-VA), illustrates pThr primed for phosphate elimination (Figure 4A, left). This structure also reveals pTyr nestled in a binding pocket stabilized by an aromatic π-stacking interaction with a nearby phenylalanine (F98) (Figure 4A, right).[13] The binding pocket also contains lysines to stabilize the negatively charged phosphate on both pThr and pTyr.[13] Although we demonstrated that there was a decrease in the ability of all phospholyases to catalyze the conversion of pThr to Dhb when tyrosine was not phosphorylated [peptide **2** (Figure 3E−H)], the total amount of Dhb accumulation for these substrates, even at short time points, was still appreciable. Therefore, we chose to further explore the requirements at the +2 position through a series of point mutations. After phospholyase incubation for 1 min, we observed no elimination for substrates in which the +2 position was substituted with charged residues (Lys and Glu for peptides **3** and **4**, respectively), polar residues (Gln for peptide **5**), or aliphatic residues (Ala and Leu for peptides **6** and **7**, respectively), as assessed by LCMS. Modest, but appreciable, levels of conversion for peptides **4**−**7** were observed after overnight incubation with SpvC, OspF, and VirA (Figure 4B). The introduction of a positive charge (Lys for peptide **3**) led to the worst overall reactivity for all of the enzymes tested, likely as a result of unfavorable interactions with the many positively charged residues already present within the enzyme active site.

However, we found that substitution with aromatic residues at the +2 position was better tolerated by the phospholyases. Although we found that His substitution at the +2 position led to negligible conversion after phospholyase incubation for 1 min (peptide **8**), we found that substitution with the aromatic residues Phe (peptide **9**) and Trp (peptide **10**) led to small but appreciable levels of phosphate elimination (1 min, Figure 4B, inset black bars). When the incubation period with phospholyase was extended to 18 h, however, near-quantitative conversion to Dhb was observed for peptides **2** and **8**−**10**. This provided further evidence of a preference for aromatic residues, with a slight decrease in the level of conversion observed for the His-substituted peptide (peptide **8**) compared to the other aromatic residues. This effect was most pronounced for HopAI compared to the other enzymes tested.

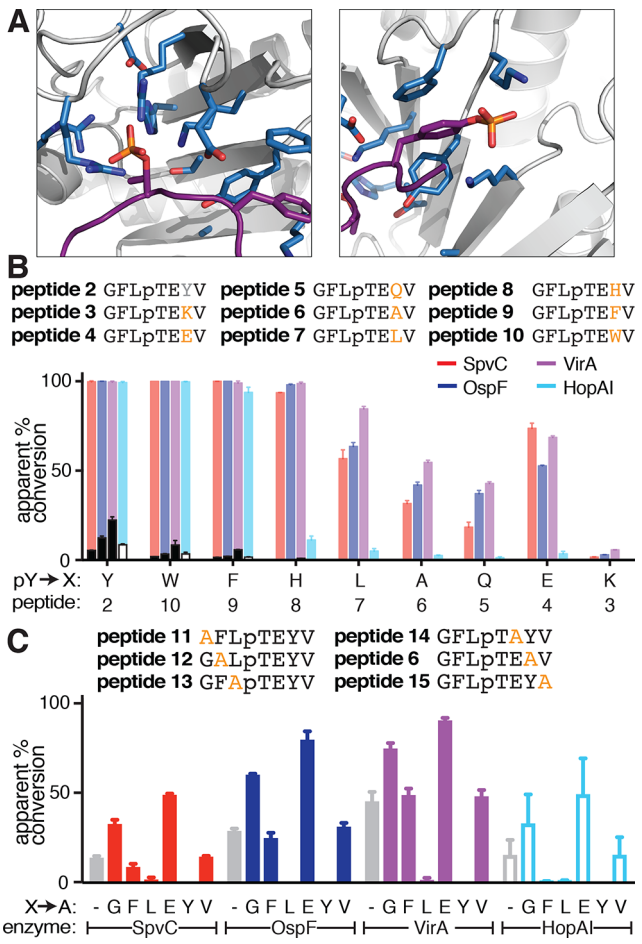

Figure 4. (A) Close-up of the ERK5 peptide (purple strand) nestled in the SpvC (blue, gray; Protein Data Bank entry 2Q8Y) binding pocket: (left) pThr poised for phosphate elimination and (right) pTyr sitting at the binding pocket stabilized by hydrogen bonds to two lysine residues and a π-stacking interaction with nearby phenylalanine. (B) Series of pThr ERK1/2 peptides possessing point mutations in the +2 position were treated for 1 min or 18 h with each phospholyase [SpvC (red), OspF (blue), VirA (purple), or HopAI (cyan)]. Inset filled bars represent the apparent conversion observed after phospholyase treatment for 1 min (for SpvC, OspF, and VirA), and inset empty bars represent the apparent conversion after treatment with HopAI for 5 min. (C) An alanine scan of peptide 2 was performed. Each alanine point mutant (peptide **6**; peptides **11**−**15**) was incubated each phospholyase for 2 min [SpvC (red), OspF (blue), and VirA (purple), solid bars] or 10 min [HopAI (cyan), empty bars]. The percent apparent conversion is reported; for reference, the apparent conversion observed for peptide **2** (gray bar) is also shown.

Exploration of Positional Sequence Requirements for Phospholyase Substrates. Our next goal was to understand the importance of other positions within the substrate as it relates to effective elimination of phosphate from the central phosphothreonine. To explore this, we prepared a small library of peptides that contained alanine substitutions in each position of peptide **2** [peptide **6**, peptides **11**−**15** (Figure 4C)]. After incubation with each phospholyase for 2 min, apparent conversion was quantified using LCMS. This analysis revealed that alanine substitution at the −1 and +2 positions (peptides **13** and **6**, respectively) led to the largest decrease in elimination relative to peptide **2** for all enzymes (Figure 4C). As previously described, the dependence for Tyr in the +2 position is unsurprising, as it is highly conserved across species and our

DOI: 10.1021/acs.biochem.8b00534
Biochemistry XXXX, XXX, XXX−XXX

earlier experiments highlight the preference for aromaticity in this position. In contrast, the −1 position is less conserved across species, consisting of predominantly hydrophobic residues Leu, Met, Trp, and Phe (Figure S5). Moreover, the crystal structure reveals that the side chain is projecting away from the enzyme without making any notable contacts. Nonetheless, our results suggest that this bulky, hydrophobic residue plays an important role in positioning the substrate for successful catalysis.

Alanine substitutions at the −2 and +3 positions (peptides **12** and **15**, respectively) led to virtually no change in the extent of elimination catalyzed by each enzyme relative to peptide **2** (Figure 4C). This result can be easily reconciled with the available crystal structure, as the side chains for both of these residues are oriented away from the enzyme and do not make contact with other sites on the enzyme or substrate. Finally, alanine substitution at the −3 and +1 positions (peptides **11** and **14**, respectively) led to a notable increase in the extent of elimination observed, as compared to that of peptide **2**, for all enzymes tested (Figure 4C). The −3 position is conserved little across species, and the crystal structure shows that the side chains in this position are again facing away from the enzyme. In the +1 position, Glu is conserved throughout many plant and mammalian MAPK activation loop sequences.[17,24] Although this residue makes hydrogen bonding contacts with active site residues in the available crystal structure, it has been previously hypothesized that smaller, more flexible amino acids lead to better catalysis at this position.[13] Our results provide support that this is indeed the case. Overall, this set of experiments demonstrates that changes in the identities of the residues flanking phosphothreonine have the potential to increase the extent of elimination catalyzed by bacterial phospholyases.

Evaluating Phospholyase-Catalyzed Elimination from Phosphoserine. Our studies thus far have suggested that there is a potential for substrate promiscuity within this family of bacterial phospholyases. Although it is generally accepted that these enzymes are capable of catalyzing elimination from phosphoserine, in addition to phosphothreonine, only a single report has tested this explicitly for OspF.[10,13] Accordingly, the ability of each phospholyase to catalyze the formation of dehydroalanine from phosphoserine-containing substrates was evaluated. To do so, we prepared phosphoserine analogues of peptide **1**, in which pSer was substituted in place of pThr [peptide **16** (Figure 5A)]. Using the same LCMS-based assay, we observed that all of the phospholyases were considerably less effective at catalyzing elimination for peptide **16** (Figure 5B, solid line) than for peptide **1** (dashed gray). SpvC was the enzyme most tolerant of the change from pThr to pSer, as 97.3 ± 0.4% apparent conversion to peptide $\mathbf{16}^{\mathbf{Dha}}$ after 3 h was observed. However, this is in stark contrast to the near-quantitative conversion of peptide **1** to peptide $\mathbf{1}^{\mathbf{Dhb}}$ catalyzed by SpvC after only 1 min. In agreement with previous findings,[10] we also observed that OspF was far less efficient at catalyzing the elimination of phosphate from pSer than from pThr. VirA and HopAI exhibited the most dramatic decreases in their abilities to catalyze the elimination of phosphate from pSer substrates, as compared to pThr substrates. Indeed, when peptide **16** was incubated with VirA, just 51.4 ± 2.7% apparent conversion was observed after 3 h, as compared to 82.9 ± 1.7% conversion for peptide **1** after 1 min. HopAI once again performed the worst of all, converting <1% of peptide **16** to peptide $\mathbf{16}^{\mathbf{Dha}}$ after 3 h. We also prepared peptide **17**, a phosphoserine analogue of peptide **2**, which lacks phosphorylation at tyrosine. Overall, we found that when peptide **17** was incubated with each of the four

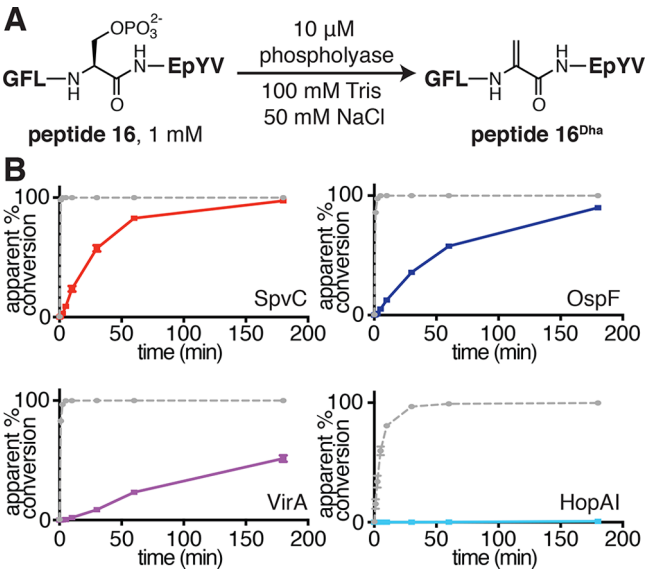

Figure 5. (A) Reaction scheme depicting the phospholyase-catalyzed elimination of phosphate from pSer-containing peptides to generate Dha-containing peptides. (B) LCMS time course assays used to monitor the conversion of peptide **16** to peptide $\mathbf{16}^{\mathbf{Dha}}$ (solid line). For each enzyme, these can be compared to the extent of conversion obtained for the pThr-containing substrate, peptide **1**, under identical conditions (dashed gray line).

phospholyases, hardly any elimination was observed, even after incubation for 3 h (Figure S6).

We next performed kinetics studies using peptide **16**, but because this substrate was suboptimal for all enzymes tested, it was possible to determine only the kinetic parameters for SpvC. We found that k_{cat} decreased by a factor of 20 and K_M increased by a factor of 8, as compared to the parameters determined for SpvC using peptide **1** (Table S2). The increase in K_M suggests that the extra methyl group on Thr, as compared to Ser, plays an important role in substrate docking. However, the large decrease in k_{cat} also suggests that this methyl group has an important mechanistic role, perhaps stabilizing charge that develops at the β-carbon during elimination. Together, these results show that the bacterial phospholyases are capable of eliminating phosphate from pSer, but far less efficiently than from pThr. However, our findings leave room for the possibility that there may be an entirely different set of requirements for pSer-containing substrates.

CONCLUSION

Bacterial phospholyases are reported to modify substrates within the MAPK family, but we lack a complete understanding of the extent of selectivity within this enzyme family. Here we have reported a study of the substrate requirements for each known phospholyase. These studies provide the first experimental validation that VirA is indeed a phosphothreonine lyase, capable of catalyzing phosphate elimination. We additionally demonstrate that OspF is the most promiscuous family member and that SpvC is the most specific for the MAPK activation loop. Notably, to infect a human host, roughly 10^3−10^5 *Salmonella* bacteria must be ingested, whereas only 10−200 *Shigella* bacteria are required.[25] This observation suggests that OspF, a more promiscuous enzyme, could contribute to the increased pathogenicity by broadly interfering with many host processes simultaneously. Our data further imply that each phospholyase

DOI: 10.1021/acs.biochem.8b00534
Biochemistry XXXX, XXX, XXX−XXX

may have its own preferred substrate and/or modify an array of substrates in host cells. Our future work will explore both of these possibilities. Thoroughly evaluating these preferences is the first step toward understanding the impact of phospholyases during bacterial infection, and toward harnessing their unique chemistry for a wide array of applications, including the identification of new biomarkers for bacterial infection and the continued development of new selective and/or bioorthogonal labeling strategies.

■ ASSOCIATED CONTENT

Supporting Information

The Supporting Information is available free of charge on the ACS Publications website at DOI: 10.1021/acs.biochem.8b00534.

Detailed experimental protocols, including conditions for the expression and purification of phospholyases, for the synthesis and purification of all peptides used, protocols for all assays used to evaluate phosphothreonine lyase activity, supplemental figures, a table of peptides used in this study, and a table summarizing all kinetics data (PDF)

■ AUTHOR INFORMATION

Corresponding Author

*E-mail: rebecca.scheck@tufts.edu.

Funding

This work was supported in part by IARPA BIC DJF.15.1200.K.0001726.

Notes

The authors declare no competing financial interest.

■ ACKNOWLEDGMENTS

The authors thank C. Czekster for helpful conversations regarding this work. The authors gratefully acknowledge D. Walt and J. Kritzer and members of the Walt and Kritzer laboratories, as well as many colleagues within the Department of Chemistry of Tufts University.

■ REFERENCES

(1) Baxt, L. A., Garza-Mayers, A. C., and Goldberg, M. B. (2013) Bacterial Subversion of Host Innate Immune Pathways. *Science 340*, 697−701.

(2) Brodsky, I. E., and Medzhitov, R. (2009) Targeting of immune signalling networks by bacterial pathogens. *Nat. Cell Biol. 11*, 521−526.

(3) Escoll, P., Mondino, S., Rolando, M., and Buchrieser, C. (2016) Targeting of host organelles by pathogenic bacteria: a sophisticated subversion strategy. *Nat. Rev. Microbiol. 14*, 5−19.

(4) Hicks, S. W., and Galan, J. E. (2013) Exploitation of eukaryotic subcellular targeting mechanisms by bacterial effectors. *Nat. Rev. Microbiol. 11*, 316−326.

(5) Reddick, L. E., and Alto, N. M. (2014) Bacteria fighting back: how pathogens target and subvert the host innate immune system. *Mol. Cell 54*, 321−328.

(6) Ribet, D., and Cossart, P. (2010) Pathogen-mediated posttranslational modifications: A re-emerging field. *Cell 143*, 694−702.

(7) Salomon, D., and Orth, K. (2013) What pathogens have taught us about posttranslational modifications. *Cell Host Microbe 14*, 269−279.

(8) Shan, L., He, P., and Sheen, J. (2007) Intercepting host MAPK signaling cascades by bacterial type III effectors. *Cell Host Microbe 1*, 167−174.

(9) Brennan, D. F., and Barford, D. (2009) Eliminylation: a post-translational modification catalyzed by phosphothreonine lyases. *Trends Biochem. Sci. 34*, 108−114.

(10) Li, H., Xu, H., Zhou, Y., Zhang, J., Long, C., Li, S., Chen, S., Zhou, J.-M., and Shao, F. (2007) The Phosphothreonine Lyase Activity of a Bacterial Type III Effector Family. *Science 315*, 1000.

(11) Mittal, R., Peak-Chew, S. Y., and McMahon, H. T. (2006) Acetylation of MEK2 and I kappa B kinase (IKK) activation loop residues by YopJ inhibits signaling. *Proc. Natl. Acad. Sci. U. S. A. 103*, 18574−18579.

(12) Zhang, J., Shao, F., Li, Y., Cui, H., Chen, L., Li, H., Zou, Y., Long, C., Lan, L., Chai, J., Chen, S., Tang, X., and Zhou, J. M. (2007) A Pseudomonas syringae effector inactivates MAPKs to suppress PAMP-induced immunity in plants. *Cell Host Microbe 1*, 175−185.

(13) Zhu, Y., Li, H., Long, C., Hu, L., Xu, H., Liu, L., Chen, S., Wang, D. C., and Shao, F. (2007) Structural insights into the enzymatic mechanism of the pathogenic MAPK phosphothreonine lyase. *Mol. Cell 28*, 899−913.

(14) Chen, L., Wang, H., Zhang, J., Gu, L., Huang, N., Zhou, J. M., and Chai, J. (2008) Structural basis for the catalytic mechanism of phosphothreonine lyase. *Nat. Struct. Mol. Biol. 15*, 101−102.

(15) Ke, Z., Smith, G. K., Zhang, Y., and Guo, H. (2011) Molecular mechanism for eliminylation, a newly discovered post-translational modification. *J. Am. Chem. Soc. 133*, 11103−11105.

(16) Neumann, C., Fraiture, M., Hernandez-Reyes, C., Akum, F. N., Virlogeux-Payant, I., Chen, Y., Pateyron, S., Colcombet, J., Kogel, K. H., Hirt, H., Brunner, F., and Schikora, A. (2014) The Salmonella effector protein SpvC, a phosphothreonine lyase is functional in plant cells. *Front. Microbiol. 5*, 548.

(17) Cargnello, M., and Roux, P. P. (2011) Activation and function of the MAPKs and their substrates, the MAPK-activated protein kinases. *Microbiol Mol. Biol. Rev. 75*, 50−83.

(18) Schmutz, C. S., Ahrne, E., Kasper, C. A., Tschon, T., Sorg, I., Dreier, R. F., Schmidt, A., and Arrieumerlou, C. (2013) Systems-Level Overview of Host Protein Phosphorylation During Shigella flexneri Infection Revealed by Phosphoproteomics. *Mol. Cell. Proteomics 12*, 2952−2968.

(19) Lippmann, J., Gwinner, F., Rey, C., Tamir, U., Law, H. K., Schwikowski, B., and Enninga, J. (2015) Bacterial Internalization, Localization, and Effectors Shape the Epithelial Immune Response during Shigella flexneri Infection. *Infect. Immun. 83*, 3624−3637.

(20) Sharma, K., D'Souza, R. C. J., Tyanova, S., Schaab, C., Wisniewski, J. R., Cox, J., and Mann, M. (2014) Ultradeep Human Phosphoproteome Reveals a Distinct Regulatory Nature of Tyr and Ser/Thr-Based Signaling. *Cell Rep. 8*, 1583−1594.

(21) Arrigoni, G., Resjo, S., Levander, F., Nilsson, R., Degerman, E., Quadroni, M., Pinna, L. A., and James, P. (2006) Chemical derivatization of phosphoserine and phosphothreonine containing peptides to increase sensitivity for MALDI-based analysis and for selectivity of MS/MS analysis. *Proteomics 6*, 757−766.

(22) Zhang, Y., Yang, R., Huang, J., Liang, Q., Guo, Y., Bian, W., Luo, L., and Li, H. (2015) Michael addition of dehydroalanine-containing MAPK peptides to catalytic lysine inhibits the activity of phosphothreonine lyase. *FEBS Lett. 589*, 3648−3653.

(23) Cheng, C., Gao, X., Feng, B., Sheen, J., Shan, L., and He, P. (2013) Plant immune response to pathogens differs with changing temperatures. *Nat. Commun. 4*, 2530.

(24) Rodriguez, M. C., Petersen, M., and Mundy, J. (2010) Mitogen-activated protein kinase signaling in plants. *Annu. Rev. Plant Biol. 61*, 621−649.

(25) Leggett, H. C., Cornwallis, C. K., and West, S. A. (2012) Mechanisms of pathogenesis, infective dose and virulence in human parasites. *PLoS Pathog. 8*, No. e1002512.

DOI: 10.1021/acs.biochem.8b00534
Biochemistry XXXX, XXX, XXX−XXX